Applied Chemical Engineering (2024) Volume 7 Issue 2
doi: 10.59429/ace.v7i2.1868

ORIGINAL RESEARCH ARTICLE

Nano-structuration influence on the polyimide-based spatial light modulator's parameters

Natalia Kamanina[1,2,3,*]

[1] *Lab for Photophysics of Nanostructured Materials and Devices, Joint Stock Company Scientific and Production Corporation Vavilov State Optical Institute, St.-Petersburg 192171, Russia; nvkamanina@mail.ru*
[2] *Department of Photonica, St.-Petersburg Electrotechnical University (LETI), St.-Petersburg 197376, Russia*
[3] *Petersburg Nuclear Physics Institute, National Research Center Kurchatov Institute, Gatchina 188300, Russia*

ABSTRACT

The classical and the nano-structured spatial light modulators (SLMs) especially based on the polyimide photosensitive layers, as the key element of the optoelectronic devices, display, and telecommunications schemes are considered. The main emphasis is placed on the device with a polyimide photo-layer due to its high sensitivity and acceptable performance. A modulator's basic characteristics are studied taken into account the comparison with the different types of the photo-layers, such as: ZnSe, ZnS, a-Si:H. Liquid crystal (LC) media is considered as the modulation system. It is indicated that the different methods and approaches are applied for investigation of the basic SLM parameters, such as: Z-scanning technique, third harmonic generation, four-wave mixing set-up, etc. In the current paper the laser holographic technique is used to investigate the resolution, sensitivity, and speed of the LC-SLM devices. The influence of the fullerene doping on the organic photo-layers based on the polyimide materials is presented. This influence of this nano-structuration process on the modulator's basic parameters is discussed.

Keywords: nano-structuration; spatial light modulator; photo-layers; polyimide; liquid crystal; resolution; sensitivity; speed; fullerene doping

ARTICLE INFO

Received: 17 April 2023
Accepted: 21 August 2023
Available online: 13 March 2024

1. Introduction

It is well known that among the basic devices used in the general optoelectronics, laser techniques, biomedicine instruments, etc. The electrically- and optically (light)-addressed spatial light modulator (SLM) is one of the key elements. It can be used in the system for the modulation and conversion of the laser beam, for the writing-reading information, for the specific hologram recording, for the activation of the optical limiting effects in order to protect the human eyes and technical devices from high irradiation, etc.[1–30]. The extended area of the SLM applications can be shown in **Figure 1**. The important prospects to use the reversible and irreversible information recording based on the features of the matrix media are considered[1–3], including the structures of chalcogenide photolayers[4,7], of the hydrogenated tellurium carbide and the amorphous hydrogenated silicon photolayers[5,10], of the polyimide materials[6,12,13]. The liquid crystal (LC) mesophase is often chosen as the modulating medium in these modulators due to its easy controllability under the external influence and the small parameters of the applied supply voltage. Different effect in the LC mesophase[14,19] and influence of the orienting layers on the LC

features[15] and use of the SLM for the holograms improvements[9,17] were shown. Moreover, the specific organic molecular crystal and classical ones were presented[16,18,26] to use them in the modulation technique area. Furthermore, novel interesting architecture of the LC structures and features of the schemes are considered[20,31–35]. It should be remembered that basically three famous schemes can be used in order to operate with the SLM structure and to predict the unique properties. Z-scanning technique, generation of the third harmonic of the laser radiation approach (third-order generation scheme), four-wave mixing technique, modulation transfer function set-up, etc. are applied. Different methods to estimate the modulator basic parameters, such as the sensitivity, speed, contract, resistivity, etc., are considered. The spatial light modulator is the device, which allows modulating the amplitude, phase or polarization of the light according to the specific tasks.

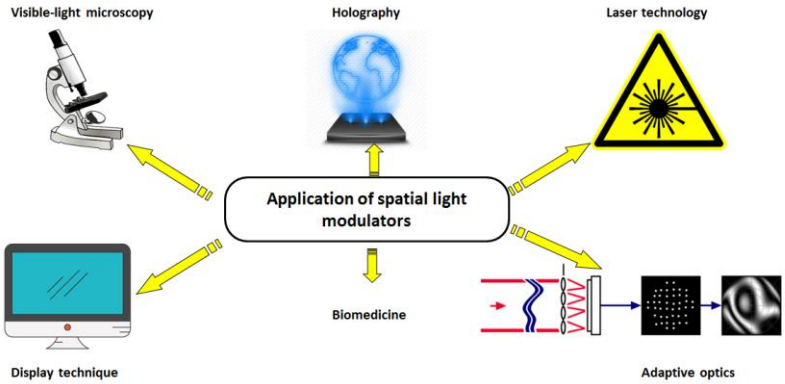

Figure 1. Visualization of the areas of the use of the spatial light modulators.

Often, the material included in the SLM, can exhibit both the recording and modulating properties at the same time. It should be mentioned, that the SLM is a complicated multilayer sandwich devise. Generally SLM consists of two glass or quartz substrates, conducting coatings, photo-layers and modulating one. The mono- or poly-crystalline compounds, organic thin films, ceramics, amorphous hydrogenated structures, etc. can be applied as the basic photosensitive layers. Among them the following systems can be used: ZnS, ZnSe, CdS, CdSe, GaAs, $As_{10}Se_{90}$, a-Si:H, a-SiC:H, polyimides, polyvinyl carbozole, pyridine, polymetil methacrylate, etc. As the basic modulating layers the potassium—dihydrogen—phosphate (KDP) and deuterated potassium dihydrophosphate (DKDP) crystals, $Bi_{12}GeO_{20}$, $Bi_{12}SiO_{20}$ (BSO), 4-N,N-dimethylamino-4′-N′-methyl-stilbazolium tosylate (DAST) organic crystal, ferroelectric ceramics, liquid crystal (LC), etc., can be used. Naturally, the specific photo- and modulating layers are selected for a specific spectral and energy ranges and can be activated by the external optical, electrical, acoustic, magnetic or thermal signal.

In order to operate at the simplified control conditions the SLMs based on the modulating liquid crystal layer are used more often. These LC-SLM structures have high sensitivity (~10^{-6}–10^{-7} J × cm^{-2}), low control voltages (units-tens of Volts), and they have not complicated manufacture and the technological process. Moreover, LC-SLM has high resolution and good time characteristics. These two parameters are always in the compromise with each other: the higher the resolution, the lower the performance, determined by the spreading rate of the potential relief created when recording information. Indeed, the potential relief (potential terrain) on a photo-layer depended on the charge carrier mobility of the photo-layers, thus it depended on the type of the photo-layers. In the simple view (please see Equation 1) the spreading time τ depends on the thickness of the photo-layer d, the mobility μ of the charge carriers, and the applied voltage V[3,5]:

$$\tau = d^2 \times \mu^{-1} V^{-1} \quad (1)$$

It should be noticed, which is very important, that the LC-SLM operates at the room temperature. For example, in order to activate the modulating KDP or DKDP crystals it is necessary to cool the electro-optical crystal to a temperature of −55 °C in order to reduce the operating voltage up to 100 V[3]. It should be noticed that at the room temperature the operating voltage for these inorganic crystals is close to 1.8 kV.

It should be mentioned that the principle of the operation of the LC-SLM modulator is as follows. A constant or alternating supply voltage is applied to the transparent electrodes. The total resistance *Z* of the photo-layer and LC layers is chosen in such a way that in the absence of the recording (writing) light, most of the voltage falls on the photo-layer, and part of the voltage falling on the LC modulating layer is less than the threshold value of the electro-optical Frederick's effect used in order to activate the LC mesophase. When the photo-layer is illuminated by the exposing radiation, its conductivity (total resistance *Z*) can be changed, resulting in a redistribution of the supply voltage between the photo-layer and the LC one. This leads to activate an electro-optical effect in the LC layer and to obtain the modulation of the reading radiation in the accordance with the law of light distribution in the photo-layer. The appropriate choice of photosensitive media (ZnSe, ZnS, CdS, $As_{10}Se_{90}$, α-CdTe, α-Si: H, α-SiC: H, polyimides, etc.) ensures the operation of the LC modulators in a wide frequency (wave length) range.

It should be remarked that two modes can be basically considered for the LC-SLM operation. Schemes, which can be used to activate the LC modulator, are titled as "transmittance mode" and the "reflectance mode". **Figure 2** shows two modes classically used for the LC-SLM operation. The process to record-read image in the "transmittance mode" is visualized in **Figure 2a**; other one is shown as the "reflectance mode" in **Figure 2b**.

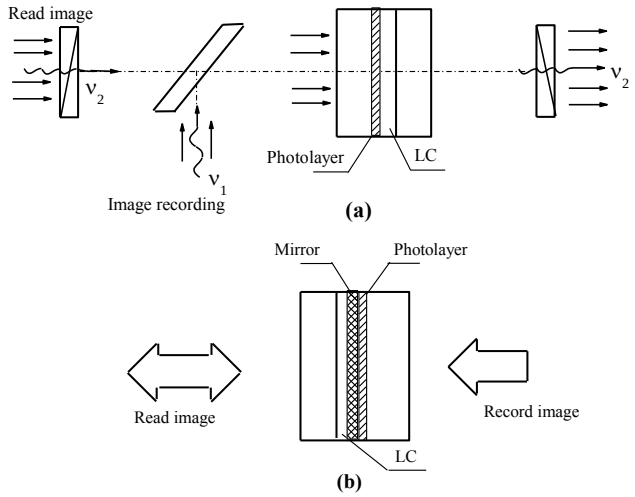

Figure 2. Some graphic presentation of the set-ups[3,36] in order to show the LC-SLM operation in the "transmittance" **(a)** and the "reflectance" modes **(b)**.

In the "reflectance mode", the reading light passes through the electro-optical crystal twice, which leads to a doubling of the phase difference and the intensity of the outgoing light. Hence, the operating voltage is decreased! However, a significant disadvantage of this scheme is the presence of the large aberrations from the large number of the interfaces in this sandwich system[3]. The wave front of the reading light is bent when it passes in both directions. The absence of the plane-parallelism of the opposite surfaces of the plates leads to multiple an internal reflections. The presence of a wedge leads to the appearance of the various types of the aberrations. Indeed, the wave front correction can be carried out, for example, by the cylindrical corrective lenses selecting. In the case of the devices operating in the "transmittance mode", these distortions are absent, since the aberrations occurring on the front surface are compensated on the back side of the structure.

The effective operation of the LC-SLM is connected with some geometric (constructions, scheme to activate the devices by the external fields) and with the physical-chemical parameters, which regarded not only to the specific native parameters of the modulators, but also depended on the modifications, for example, via nano-structuring of the interface, photo layer or modulating compound[9,13,28–46].

So, it should be clarified why the study of the parameters of the classical or modified SLMs is so important? The fact is that new materials, including metamaterials, novel operational schemes of the exposure to the photo layers, including terahertz exposure, extended fields of the application, including biomedicine, are in increasing demand and show the evidence of the improvement of their characteristics.

In the current paper the comparative SLM parameters are shown. The advantage of the nano-structuring is considered in order to improve the basic parameters of the LC-SLM based namely on the polyimide photosensitive layer and nematic LC modulation one because the polyimide layers showed the highest resolution, which is very important to test, for example, the blood cells or the DNA structures for the biomedicine applications, as for example, which were previously shown in papers by Kamanina[47] and Kamanin and Kamanina[48] for the LC cells with the polyimide orienting layers.

2. Method and materials

As has been mentioned above the SLMs had a typical structure. It was operated in the "transmittance" mode. The photo-layers were the polyimide, sensitized polyimide, ZnS, ZnSe and a-Si:H structure. The LC modulation layer was the mixture of 4′-Pentyl-4-biphenyl-carbonitrile materials (Sigma-Aldrich Co.).

To investigate the SLM characteristics the holographic technique was used; the scheme was analogous to that shown in the study of Kamanina and Vasilenko[49]. Nanosecond Nd-pulsed laser with the conversion of the first harmonic to the second one was used. The LiF passive laser crystal was used to transfer the general irradiation to the pulsed one. To clarify the experimental scheme in details, for the better understanding, this one is shown in **Figure 3**.

One can see from **Figure 3** (the general scheme that was applied) that the laser beams converted to the second harmonic passed the M1 mirror with a reflection of almost 99.9%, were then divided by the BS dividing plate into two parts; one beam passed from the first face of the plate, the second was reflected from the M2 mirror. The ratio of starts incident on the modulator (SLM) was 1:1. Behind the lens L the responses were recorded in the first diffraction order in the Raman-Nath diffraction conditions. This means that the period of the recorded lattice (the inverse of the spatial frequency) must be greater than the thickness of the medium being tested. Photodiodes PD1, PD2 provided information about the falling and the past laser beams to correct the measurements. The He-Ne laser was used as an additional in order to read the information, if the regime was changed from the reversible mode to the irreversible one. But it should be mentioned that the diffraction efficiency η was usually measured in the self-diffraction mode (reversible mode).

It is worth emphasizing once again why the holographic technique was used? The method close to the four-wave displacement of the laser beams allows to exam the material without the basis structure destroying, the step by step, that is, the pulse by pulse. This makes it possible to fix and further to calculate many physical parameters of the studied complicated sandwich system. This is an advantage, say, over the use of the destructive method of the third harmonic generating approach, for example. It should be mentioned, that via the holographic set-up the researchers can estimate the change of the diffraction efficiency at the large range of the spatial frequencies that permits to observe the dynamic change of the refractivity at the diffusion and drift process for charge carrier moving.

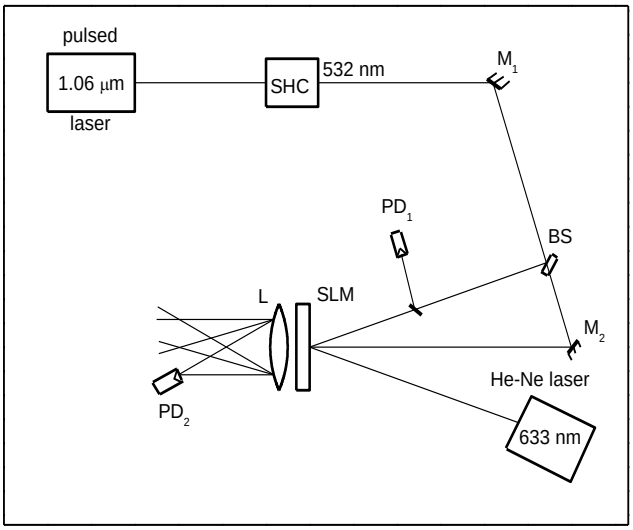

Figure 3. Some view of the experimental set-up used in the current experiments to study the SLM characteristics[49].

The matching conditions were fulfilled for the laser and the supply voltage pulses. It should be noticed, that the delay D between the laser pulse with the energy density of W_{input} and the voltage pulse with the pulse width of τ_{sup} was varied. For example, **Figure 4** presents the following dependence for the LC-SLM based on the polyimide PI photo-layer. One can testify that the best results have been obtained for the delay placed in the range 1–5 ms. It should be mentioned that the standard deviation was less than 1%–2%.

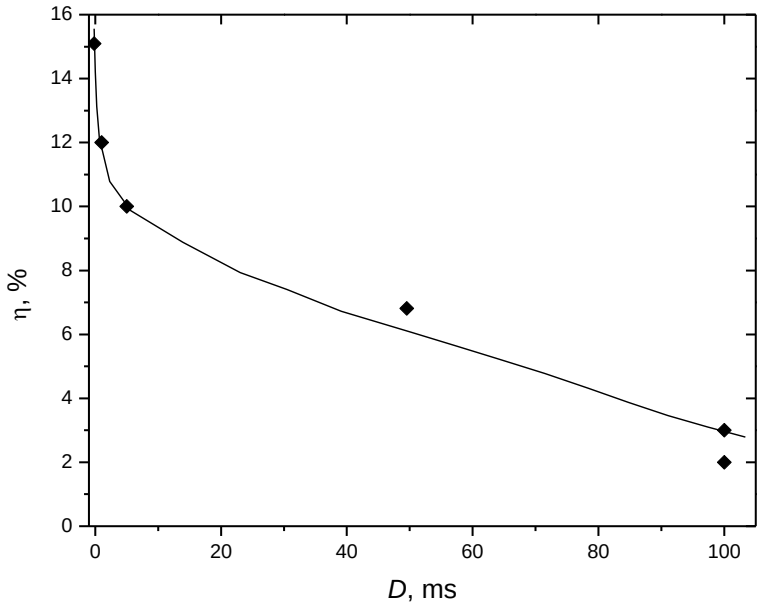

Figure 4. Dependence of the diffraction efficiency on time delay between the laser pulse and supply voltage pulse. $\Lambda = 100$ mm^{-1}, $W_{input} = 400$ μJ × cm^{-2}, supply voltage amplitude $A = 60$ V, $\tau_{sup} = 50$ ms, $T = 1$ Hz.

Under the Raman-Nath diffraction conditions, a thin amplitude-phase holographic grating was recorded by the second harmonic ($\lambda = 532$ nm) of the pulsed Nd-laser (pulse width of 20 ns) on the photo-layer. The chosen laser regime was according to which the relation was correct: $\Lambda^{-1} \geq d$, where Λ^{-1} is the inverse spatial frequency of the recording (i.e., the period of the recorded grating) and d is the film thickness.

A spatial frequency Λ was varied from 50 mm^{-1} to 700 mm^{-1}. An energy density of the irradiation incident upon the photo-layer lays in the range from 100 μJ × cm^{-2} to 2 mJ × cm^{-2}. The supply voltage pulses

were rectangular in the shape. They had amplitude of 10–60 V; a repetition frequency (*T*) of 0.5–10 Hz; their pulse width τ was varied from 20 ms to 100 ms.

It should be mentioned once again that the delay *D* between the laser and supply voltage pulses was controlled, that allowed a time lag of the structure to be taken into account and the write-readout regime to be optimized. *D* was varied from 5 μs to 50 ms. The optimal regime made possible the enhancement of the SLM speed without essential sacrifice of the SLM resolution. The holographic grating recorded was read out in the self-diffraction mode or by the collimated beam of a CW He-Ne laser with a power density of 100 μWcm^{-2}. The photo response was registered in the first diffraction order in the focal plane of the lens located behind the LC-SLM. The diffraction efficiency η was estimated via the measurement of the intensity in the first and zero diffraction. CW He-Ne laser was used in order to check and visualize the grating in the irreversible mode. In this case the energy density used to form the grating was exceeded 0.5–0.6 $J \times cm^{-2}$. At this high value of the energy density the thermal affect is included into the recording regime as one of the physical mechanism. Some image of the grating imprinted in the photo layer (in the irreversible mode) based on the polyimide is shown in **Figure 5**.

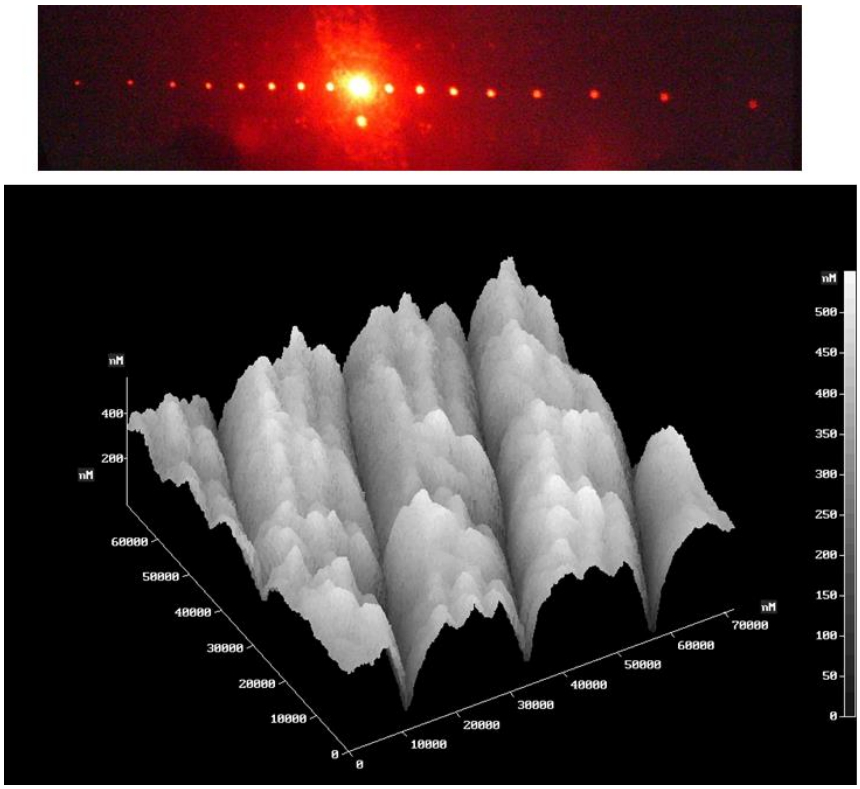

Figure 5. Optical microscopy view (upper part of the picture) and ASM-image (the lower part of the picture) of the recorded grating obtained in the irreversible mode.

Since the results obtained aim to show both the effect of photo-layer sensitization on the modulator parameters, and the difference between polymer photo-layers, due to their excellent resolution, from other photo-layers, the emphasis should be placed on the method of preparing the photo-layer on the sensitized polyimide. In this case the polyimide films were prepared from 3–6.5% PI solutions in tetrachloroethane by the centrifugal method. The films were modified by adding fullerenes C_{60} and C_{70} with the concentrations changed from 0.2 to 0.5 wt.% relative to the photosensitive polymer component. The film thickness was varied within 2–4 micrometers. (One should remember that the basic grating was recorded at the spatial

frequency of 100 mm^{-1}, thus the period of the grating is approximately of 10 micrometers). It should be noticed that both the polymer and the fullerenes are well soluble in tetrachloroethane, which provided for the obtaining of the homogeneous films with high stability under laser irradiation. The polymer films have been placed onto glass substrates (crown K8) covered with the transparent conducting layers based on the ITO (indium-tin-oxides) contacts. It should be noticed why namely the polyimide materials have been chosen to dope them with the fullerenes? It is due to the fact that polyimide structure is the system with the initial *intra*molecular donor-acceptor interaction. The acceptor fragment of the polyimide has the electron affinity energy close to 1.14–1.4 eV. When the fullerenes, as the intermolecular effective acceptor (with the electron affinity energy of 2.65–2.7 eV) have been introduced in the polyimide, the inter molecular charge transfer process can be activated. This one can be supported by the photoconductive, mass-spectrometry, spectral analysis and via the appearance of the high frequency Kerr effect in it. The efficiency of the polyimide doping process and the prediction to use it for the LC-SLM operation was previously shown in the study of Kamanina[50].

3. Results and discussion

The basic parameters of the studied LC-SLM with the different photo-layers are shown in **Table 1**. The sensitivity *S* was estimated by the energy density required to achieve 1% of the diffraction efficiency η. Time-on and time-off parameters were measured at the waveform response from the 0.1 level to 0.9 level and from the maximum of the response to 0.1 its level respectively.

Table 1. Comparative basic parameters of the LC-SLM with the different photo-layers.

Photo-layer types	η_{max} **(at** Λ**)**	***S*, μJ × cm^{-2}**	t_{on}**, ms**	t_{off}**, ms**
Pure PI	15 (at 100)	5×10^{-6}	20	500
Pure PI	10 (at 150)	~5×10^{-6}	10	300
PI + 0.2 wt.% C_{70}	17 (at 100)	5.5×10^{-6}	10	100
PI + 0.2 wt.% C_{70}	12 (at 150)	5.3×10^{-6}	8–10	90
PI + 0.5 wt.% C_{70}	16–17 (at 100)	5.7×10^{-6}	5–8	60
ZnS	10 (at 50)	2.5×10^{-6}	5	30
ZnSe	10 (at 50)	2×10^{-6}	5–7	50
a-Si:H	5–7 (at 50)	2×10^{-4}	1–3	10

One can see from **Table 1** that the highest diffraction efficiency η at the reasonably high spatial frequencies Λ (100 mm^{-1}) was obtained for SLM with the organic polyimide photo-layer. There are two probable reasons for the high resolution of the LC SLM based on polyimide. Firstly, it should be remarked that the carrier mobility of polyimide is 10^{-5}–10^{-8} $cm^2 \times V^{-1}s^{-1}$[12]. Thus, the charge carriers are spreading very slowly when the holographic grating is recorded. The spreading time can be about 20 ms and larger. By choosing the delay between the laser and supply voltage pulses, a compromise between high resolution and short switching times can be possibly reached. Second, the polyimide photo-layer, which was used in the present work, was sensitized with the *inter*molecular acceptor based on fullerene C_{70} with the higher electron affinity energy than the one for the *intra*molecular polyimide acceptor (diimide one). It predicts the increase of the polarizability of the polyimide media[51,52] and, as a result, it provokes the decrease of the time parameters.

It should be clarified a little bit that one can observe some difference between the parameters of the pure PI shown in first and second lines of **Table 1**. It is due to the fact that at large spatial frequencies (short periods of recorded grating) the dominating process for the charge transfer is diffusion; in opposite case it is drift[53]. Thus, the mechanism of the charge carrier moving can be a little bit different that influences on the main SLM parameters via the photo-layers used.

Moreover, the increase of the fullerene C_{70} content can slightly increase the sensitivity due to the reason that the photoconductivity slightly increases in this range of the fullerene C_{70} content, see **Figure 6**. It is worth clarifying that the same dependence was obtained if the polyimides and fullerenes were dissolved in the chloroform, then solutions were mixed in the selected concentrations and the films were sprayed by the centrifugation with the subsequent measurement of the photoconductive parameters.

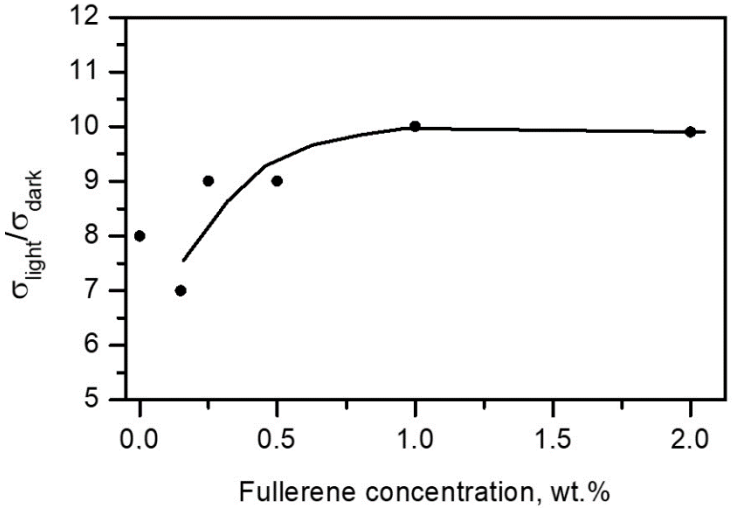

Figure 6. Dependence of the relative value of the conductivity of the polyimide photo-layer on the fullerene C_{70} content.

It should be remarked that the estimation of the conductivity was made via the mathematical procedure shown in Equation (2) accepted from the book by Gutman and Lyons[54].

$$\mu = 10^{13}\frac{jd^3}{\varepsilon V^2} \quad (2)$$

Here μ is the charge carrier mobility; *j* is the current density; *d* is the film thickness; *V* is the applied bias voltage; ε is the dielectric constant.

It should be drawing the attention once again namely for the polyimide photo-layer. This shows that the polyimide photo-layers (used for the modulator operation) have the unique advantage and it was not chosen for nanoparticles modification by chance. This material allows one to significantly shift the spectral parameters to the IR region when the nano-objects introducing; it is thermally stable and stores recorded information for quite a long time; it is good candidate to activate the charge transfer complex formation process, that predict the improvement of the basic SLM parameters. So many times these photo-layers were treated in the different mode and obtained good results.

As an additional data about the change the polyimide properties in order to make the novel composite photo-layer, the SEM-image is established. It predicts the good coinciding condition for the doping process. SEM–image data are shown in **Figure 7**.

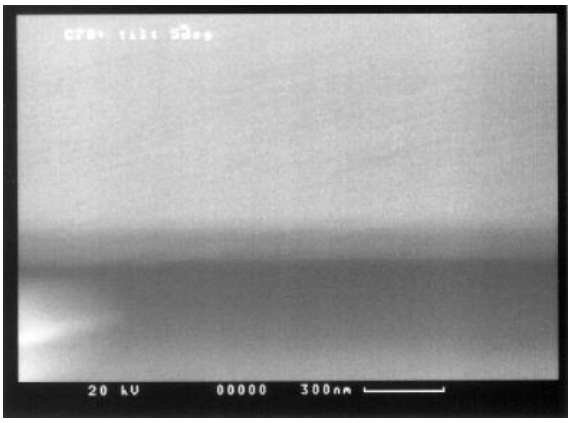

Figure 7. The image obtained on an electronic scanning microscope of the cross-section of a polyimide film with 0.2 wt.% C_{70} (light area) applied to a glass substrate (dark area).

It should be clarified that the data shown in the study of Kamanina et al[51,52] are coincided with the improvement of the characteristics not for the SLM device, but namely for the polyimide photo-layers doped with the nanoparticles. But in the current paper this evidences are included in the SLM operation in order to improve the sensitivity, speed and resolution as the mail SLM features. Moreover, it should be remarked that up to now so many scientific team search for the ways to find the compromise between the resolution and speed of the SLM, test the novel area of the SLM applications, study the influence of the operation scheme regime on the parameters of the SLM, etc.[53–58]. Thus, the results of the current paper can extend some area of the material science useful for the SLM characteristics investigation and applications, including the nano-structuration process.

The polyimide structures properties change can be considered via the comparison of the some results for the doped polyimide presented in the current paper and with the data obtained of other scientific groups for the polyimide materials. In paper written by Du et al.[59] the researchers were used UV irradiation to change the contact angle at the polyimide surface due to the ultraviolet laser direct texturing. It is coincided with our results. Really, the skeleton of the fullerene molecules influence on the surface wetting features. For our doped polyimide we have established the following link for the contact angle: 90–91 (pure polyimide), 93–94 (0.2 wt.% C_{70} doped), 95–96 (0.5 wt.% C_{70} doped). Thus, the sensitization process (our approach) and the UV structuring[59] predicted the change of the surface via the visualization of the contact (wetting) angle. In the paper written by Cherkashina et al.[60] the polyimide structured with the WO_2 component was tested with the application of the electron irradiation. The increase of the mechanical properties of the PI-WO_2 composite was established. It is coincided with the testing of the mechanical parameters for our PI-C_{70} structure as well, which increase the microhardness on 5%. It is worth saying that comparing different methods is most likely not entirely true. However, a simple comparison based on the observation of a trend in improving the properties of matrix polyimide during the surface doping or the texturing suggests that this process changes the properties of the polyimide.

Regarding the value of the basic parameters of the ZnS, ZnSe and a-Si:H photo-layers it should be taken into account the following reasons. The peak of the spectral sensitivity, for example of the ZnSe films lies in the range of 450–480 nm. Therefore, writing the grating was not the most favorable at the wavelength of 532 nm, which is not coincided with the range of the spectral sensitivity of the ZnSe photo-layer. The relatively high value of the diffraction efficiency (about 10%) is perhaps explained by the availability of a long-wave tail of the optical absorption. The same evidences can be possible for the explanation for the ZnS photo-layer, but its operation can be extended from 400 nm to 800 nm with good advantage, which revealed the better sensitivity at the wavelength of 532 nm. Concerning the a-Si:H photo-layer it should be told that the potential relief was partially erased by the readout beam of the He—Ne laser at the wavelength of 632 nm. Thus, the

"transmittance" mode is not good to study the SLM based on this layer, the mirror should be placed between photo-layer and LC one in order to avoid the influence of the reading beam on the photo layer. But, the dynamic characteristics of the LC SLM with the a-Si:H photo-layer were the better due to high charge carrier mobility of this structure. Nevertheless, it is quite obvious to compare the basic characteristics of the modulators with the different photo-layers. This allows one to more clearly view the advantages and disadvantages of each device with different methods of testing it.

Furthermore, it should be said that currently, due to the use of the different nanostructures, it is possible to create modulators devices in which the functions of both recording and read-outing layers will be performed by one material. This is possible, for example, when using such effective nanostructure as the graphene, graphene oxides, reduced graphene oxides, Ag NPs, etc.[61–65]. Furthermore, the polymer-dispersed spatial light modulators with the nanostructured layers or the interface, with some unique experimental conditions, etc. can be considered as well[66,67].

4. Conclusion

To summarize the showed results it should be firstly testify that the unique holographic set-up were used to study the basic LC-SLM parameters. The main electro-optical characteristics of the light-addressed liquid-crystal spatial light modulators with various photosensitive layers (ZnSe, ZnS, a-Si:H, polyimide) were comparatively studied by this technique using the "transmittance" mode. The resolution, sensitivity and speed parameters were taken into account. It should be noticed that the LC SLM based on the polyimide photo-layer was demonstrated the highest resolution. It was estimated at the spatial frequencies of 100 and 150 mm^{-1}, at which the sensitivity was found in the range of 5.7×10^{-6}–5.3×10^{-6} $\mu J \times cm^{-2}$. Thus the efficiently of the doping process for the polyimide materials was supported. Unfortunately, the speed of the device based on the polyimide photo-layer is not so good, in comparison with that for the semiconductor's photo-layers. The effect was conditioned by the low charge carrier mobility in the polyimide structure, which can reveal slow spreading the potential relief created at the photo-layer-LC interface. Due to higher charge carrier mobility in the ZnSe, ZnS, a-Si:H materials it was shown the better their dynamic characteristics.

It is worth noting that in an addition to the design of the modulator (its scheme of operation for "transmittance" or "reflection", the holographic or the modulation transfer function techniques, etc.), to the choice of the photo-layer and the modulating medium, it is quite obvious that the doping of the photo-layer with nanoparticles causes the modification of the main parameters of the LC-SLM.

The results obtained can extend the area of the application of the LC-SLM, not only for the optoelectronics use, but for the biomedicine and education process applying. This is very significant for young researchers to actually see the recording of the amplitude-phase holograms on the organic photo-layers of the light modulators. Based on the teaching practice at the Electrotechnical University of the author of this article, it is important for students and postgraduates to see the visual physical effects obtained when working in the field of the materials science.

Indeed, so many experiments can be involved in future for this perspective direction. XRD spectra, ellipsometry data, SEM analysis, comparative data established not only by the holographic recording technique, but by Z-scanning scheme, third harmonic generation, etc. can be made. But, it will be considered in future, these data will be shown in the other paper, not in this one.

Acknowledgments

The authors would like to acknowledge her colleagues: F. Kajzar and Ch. Andraud (France), D.P. Uskokovic (Serbia); V.I. Studenov and S.A. Serov (Russia) for their help in this study at its different steps. Moreover, the

results have been discussed in Vincha Institute (Belgrade, Serbia) on 2017 and they have been visualized as the Plenary Lectures in Cluster conferences (Ivanovo, Russian Federation) on 2016, 2018, 2021 and in Nanotechnology section in Ariel University (2008, 2010, 2012, 2014, 2016, Ariel, Israel). The presented here results are coincided with the main research directions of the Lab for Photophysics of media with nanoobjects (Vavilov State Optical Institute) and they are the some analysis of the part of a work supported partially by Russian Foundation for Basic Research, grants No.10-03-00916 (2010–2012), No.13-03-00044 (2013–2015) as well as by FP7 Marie Curie International researchers exchange proposal "BIOMOLEC" (2011–2015). Some recently obtained data have been shown in the scientific conference in Bolshie Kotyu (Bajkal, Siberian region), organized by the Irkutsk State University on July 2022 and in Applied Optics conference (Vavilov State Optical Institute, Nanotechnology section, December 2022, Saint-Petersburg, Russia).

Conflict of interest

The author declares no conflict of interest.

References

1. Petrov MP, Stepanov SI, Khomenko AV. *Photosensitive Electrooptical Media for Holography and Optical Information Processing* (Russian). Nauka; 1983. 268p.
2. Hauck R, Bryngdahl O. Computer-generated holograms with pulse-density modulation. *Journal of the Optical Society of America A* 1984; 1(1): 5–10. doi: 10.1364/JOSAA.1.000005
3. Vasil'ev AA, Casasent D, Kompanets LN, et al. *Spatial Light Modulators* (Russian). Radio i Svyaz'; 1987. 320p.
4. Groznov MA, Kamanina NV, Myl'nikov MS, et al. Optical homogeneity of light modulators of the chalcogenide vitreous semiconductor—Liquid crystal type. *Soviet Journal of Optical Technology* 1989; 56(5): 267–268.
5. Dumarevskii YuD, Zakharova TV, Kovtonyuk NF, et al. Characteristics of liquid-crystal optically controlled transparencies based on a-CdTe and a-Si:H photosensitive layers. *Soviet Journal of Optical Technology* 1989; 56: 729–732.
6. Kamanina NV, Soms LN, Tarasov AA. Correction of phase aberrations by the holographic method using liquid-crystal spatial light modulators. *Optics and Spectroscopy* 1990; 68(3): 403–404.
7. Godya SI, Danilyuk SA, Ermakov AS, et al. Liquid crystal space-time light modulators with thin zinc selenide films. *Soviet Physics Technical Physics* 1991; 61: 349–351.
8. Aleksandrov BG, Nikitin VV, Kuz'mina II, et al. Measurement of the dynamic characteristics of optically addressed spatial light modulators. *Soviet Journal of Optical Technology* 1992; 59: 75–77.
9. Vladimirov FL, Chaika AN, Morichev IE, et al. Temporal characteristics of optically controlled transparencies of the photoconductor—Liquid crystal type used as holographic correlators. *Soviet Journal of Optical Technology* 1993; 60: 483–486.
10. Ivanova NL, Kamanina NV, Komarov AP, et al. Optimization of the dynamic characteristics of space-time light modulators with an a-Si:H photolayer. *Technical Physics Letters* 1993; 19(4): 216–218.
11. Belyaev VV, Chigrinov VG. Figure of merit of liquid crystal materials for optically addressed spatial modulators. *Applied Optics* 1993; 32(2): 141–146. doi: 10.1364/AO.32.000141
12. Mylnikov VS. *Photoconducting Polymers*. Springer-Verlag; 1994. 88p.
13. Kamanina NV. Using the operator Laplace method to estimate the response time of space-time light modulators. *Technical Physics* 1994; 39(1): 83–85.
14. Blinov LM, Chigrinov VG. *Electrooptic Effects in Liquid Crystal Materials*. Springer; 1994. 459p.
15. Kamanina NV, Vasilenko NA. Effect of various alignment films on dynamic characteristics of LC spatial light modulators. *Proceedings of SPIE* 1996; 2731: 220–226. doi: 10.1117/12.230665
16. Meier U, Bösch M, Bosshard C, Günter P. DAST a high optical nonlinearity organic crystal. *Synthetic Metals* 2000; 109(1–3): 19–22. doi: 10.1016/S0379-6779(99)00190-3
17. Coomber SD, Cameron CD, Hughes JR, et al. Optically addressed spatial light modulators for replaying computer-generated holograms. In: Proceedings Volume 4457, Spatial Light Modulators: Technology and Applications; 8 November 2001; San Diego, CA, United States. Volume 4457. pp. 9–19.
18. Follonier S, Fierz M, Biaggio I, et al. Structural, optical, and electrical properties of the organic molecular crystal 4-N,N-dimethylamino-4'-N'-methyl stilbazolium tosylate. *Journal of the Optical Society of America B* 2002; 19(9): 1990–1998. doi: 10.1364/JOSAB.19.001990
19. Birch P, Young R, Chatwin C, et al. Fully complex optical modulation with an analogue ferroelectric liquid crystal spatial light modulator. *Optics Communications* 2000; 175(4–6): 347–352. doi: 10.1016/S0030-4018(00)00478-8

20. Jesacher A, Schwaighofer A, Fürhapter S, et al. Wavefront correction of spatial light modulators using an optical vortex image. *Optics Express* 2007; 15(9): 5801–5808. doi: 10.1364/OE.15.005801
21. Kelemen L, Ormos P, Vizsnyiczai G. Two-photon polymerization with optimized spatial light modulator. *Journal of the European Optical Society* 2011; 6: 11029. doi: 10.2971/jeos.2011.11029
22. Fan F, Du T, Srivastava AK, et al. Axially symmetric polarization converter made of patterned liquid crystal quarter wave plate. *Optics Express* 2012; 21(20): 23036–23043. doi: 10.1364/OE.20.023036
23. Huang SY, Zheng HY, Yu KY, et al. Electrically tunable prism grating based on a liquid crystal film with a photoconductive layer. *Optical Materials Express* 2012; 2(12): 1791–1796. doi: 10.1364/OME.2.001791
24. Sun J, Chen Y and Wu ST. Submillisecond-response and scattering-free infrared liquid crystal phase modulators. *Optics Express* 2012; 20(18): 20124–20129. doi: 10.1364/OE.20.020124
25. Song Z, Yu Y, Zhang X, et al. Optical microfiber phase modulator directly driven with low-power light. *Chinese Optics Letters* 2014; 12(9): 090606. doi: 10.3788/COL201412.090606
26. Cai L, Mahmoud A, Khan M, et al. Acousto-optical modulation of thin film lithium niobate waveguide devices. *Photonics Research* 2019; 7(9): 1003–1013. doi: 10.1364/PRJ.7.001003
27. Uthayakumar M, Saraswathi V, Pasupathi G, et al. Structural, third-order nonlinear optical properties and optical limiting studies of novel zinc potassium aluminum sulfate nonadecahydrate single crystal. *Journal of Materials Science: Materials in Electronics* 2020; 31: 22522–22533. doi: 10.1007/s10854-020-04763-z
28. Jeyaram S. Intermolecular charge transfer in donor—Acceptor substituted triarylmethane dye for NLO and optical limiting applications. *Journal of Materials Science: Materials in Electronics* 2021; 32: 9368–9376. doi: 10.1007/s10854-021-05600-7
29. Jajszczyk A. Optical networks—The electro-optic reality. *Optical Switching and Networking* 2005; 1(1): 3–18. doi: 10.1016/j.osn.2004.11.002
30. van Putten EG, Vellekoop IM, Mosk AP. Spatial amplitude and phase modulation using commercial twisted nematic LCDs. *Applied Optics* 2008; 47(12): 2076–2081. doi: 10.1364/AO.47.002076
31. Sun Z, Zheng Y, Fu Y. Graphene-based spatial light modulator using metal hot spots. *Materials* 2019; 12(19): 3082. doi: 10.3390/ma12193082
32. Hsu WF, Weng MH. Compact holographic projection display using liquid-crystal-on-silicon spatial light modulator. *Materials* 2016; 9(9): 768. doi: 10.3390/ma9090768
33. Mahafzah BA, Al-Adwan AA, Zaghloul RI. Topological properties assessment of optoelectronic architectures. *Telecommunication Systems* 2022; 80(4): 599–627. doi: 10.1007/s11235-022-00910-5
34. Kozacki T, Chlipala M, Martinez-Carranza J, et al. LED near-eye holographic display with a large non-paraxial hologram generation. *Optics Express* 2022; 30(24): 43551–4365. doi: 10.1364/OE.468823
35. Seki A, Shimizu K, Aoki K. Chiral π-conjugated liquid crystals: Impacts of ethynyl linker and bilateral symmetry on the molecular packing and functions. *Crystals* 2022; 12(9): 1278. doi: 10.3390/cryst12091278
36. Kamanina NV. Electrooptical systems based on the liquid crystals and fullerenes—Perspective materials of the nanoelectronics. Properties and area of the applications. Textbook for masters. IFMO University Press; 2008. 136p.
37. Heo J, Huh JW, Yoon TH. Fast-switching initially-transparent liquid crystal light shutter with crossed patterned electrodes. *AIP Advances* 2015; 5: 047118. doi: 10.1063/1.4918277
38. Lin GJ, Chen TJ, Lin YT, et al. Effects of chiral dopant on electro-optical properties of nematic liquid crystal cells under in-plane switching and non-uniform vertical electric fields. *Optical Materials Express* 2014; 4(12): 2468–2477. doi: 10.1364/OME.4.002468
39. Macfaden AJ, Wilkinson TD. Characterization, design, and optimization of a two-pass twisted nematic liquid crystal spatial light modulator system for arbitrary complex modulation. *Journal of the Optical Society of America A* 2017; 34(2): 161–170. doi: 10.1364/JOSAA.34.000161
40. Clark NA, Lagerwall ST. Submicrosecond bistable electro‐optic switching in liquid crystals. *Applied Physics Letters* 1980; 36(11): 899–901. doi: 10.1063/1.91359
41. Wahle M, Kasdorf O, Kitzerow HS, et al. Electrooptic switching in graphene-based liquid crystal cells. *Molecular Crystals and Liquid Crystals* 2011; 543(1): 187–193. doi: 10.1080/15421406.2011.569524
42. Honma M, Miura M, Nose T. Liquid-crystal-grating-based optical displacement sensors. *Applied Optics* 2016; 55(35): 10045–10052. doi: 10.1364/AO.55.010045
43. Likhomanova SV, Kamanina NV. COANP-fullerenes system for optical modulation. *Journal of Physics: Conference Series* 2016; 741: 012146. doi: 10.1088/1742-6596/741/1/012146
44. Belyaev VV, Solomatin AS, Chausov DN, et al. optical properties of composite heterophase objects with liquid crystal material for different display applications. *Journal of the Society for Information Display* 2017; 25(9): 561–567. doi: 10.1002/jsid.606
45. Kamanina NV. Nanoparticles doping influence on the organics surface relief. *Journal of Molecular Liquids* 2019; 283: 65–68. doi: 10.1016/j.molliq.2019.03.043
46. Kamanina NV, Toikka AS, Zvereva GN, et al. Surface relief of polyimide thin-film orienting materials for liquid crystalline light modulators (Russian). *Liquid Crystals and their Application* 2021; 21(4): 47–52. doi: 10.18083/LCAppl.2021.4.47

47. Kamanina NV. Similarities and differences between the effect of orientation of red blood cells in a nematic liquid-crystal medium and the Fröhlich electrical vibrations. *Technical Physics Letters* 1997; 23(12): 902–905. doi: 10.1134/1.1261926
48. Kamanin AA, Kamanina NV. Erythrocyte induced structurization of a liquid crystal mesophase. *Technical Physics Letters* 2006; 32(7): 610–613. doi: 10.1134/S1063785006070182
49. Kamanina NV, Vasilenko NA. Influence of operating conditions and of interface properties on dynamic characteristics of liquid-crystal spatial light modulators. *Optical and Quantum Electronics* 1997; 29(1): 1–9. doi: 10.1023/A:1018506528934
50. Kamanina NV. Mechanisms of optical limiting in π-conjugated organic system: Fullerene-doped polyimide. *Synthetic Metals* 2022; 127(1–3): 121–128. doi: 10.1016/S0379-6779(01)00598-7
51. Kamanina NV, Uskokovic DP. Refractive index of organic systems doped with nano-objects. *Materials and Manufacturing Processes* 2008; 23(6): 552–556. doi: 10.1080/10426910802157722
52. Kamanina NV, Emandi A, Kajzar F, et al. Laser-induced change in the refractive index in the systems based on nanostructured polyimide: Comparative study with other photosensitive structures. *Molecular Crystals and Liquid Crystals* 2008; 486(1): 1–11. doi: 10.1080/15421400801914319
53. Kamanina NV. The effect of the charge transfer pathway during intermolecular complex formation on nonlinear optical and photoconducting properties of nanocomposites. *Technical Physics Letters* 2012; 38(2): 114–117. doi: 10.1134/S1063785012020083
54. Gutman F, Lyons LE. *Organic Semiconductors* (Russian). John Wileys & Sons; 1967. 858p.
55. Rout S, Sonkusale S. Wireless multi-level terahertz amplitude modulator using active metamaterial-based spatial light modulation. *Optics Express* 2016; 24(13): 14618–14631. doi: 10.1364/OE.24.014618
56. Zhang Y, Ren Y, Chen J, et al. Fast testing of partial camera lenses based on a liquid crystal spatial light modulator. *Applied Optics* 2022; 61(22): 6420–6429. doi: 10.1364/AO.460384
57. Alaloul M, Khurgin JB, Al-Ani I, et al. On-chip low-loss all-optical $MoSe_2$ modulator. *Optics Letters* 2022; 47(15): 3640–3643. doi: 10.1364/OL.465171
58. Shcherbin K, Gvozdovskyy I, Shumelyuk A, et al. Near-infrared sensitive two-wave mixing adaptive interferometer based on a liquid crystal light valve with a semiconductor substrate. *Applied Optics* 2022; 61(22): 6498–6503. doi: 10.1364/AO.465085
59. Du Q, Ai J, Qin Z, et al. Fabrication of superhydrophobic/superhydrophilic patterns on polyimide surface by ultraviolet laser direct texturing. *Journal of Materials Processing Technology* 2018; 251: 188–196. doi: 10.1016/j.jmatprotec.2017.08.034
60. Cherkashina NI, Pavlenko VI, Abrosimov VM, et al. Effect of 10 MeV electron irradiation on polyimide composites for space systems. *Acta Astronautica* 2021; 184: 59–69. doi: 10.1016/j.actaastro.2021.03.032
61. Sorianello V, Midrio M, Contestabile G, et al. Graphene—Silicon phase modulators with gigahertz bandwidth. *Nature Photonics* 2018; 12(1): 40–44. doi: 10.1038/s41566-017-0071-6
62. Gan X, Zhao C, Wang Y, et al. Graphene-assisted all-fiber phase shifter and switching. *Optica* 2015; 2(5): 468–471. doi: 10.1364/OPTICA.2.000468
63. Wang Y, Gan X, Zhao C, et al. All-optical control of microfiber resonator by graphene's photothermal effect. *Applied Physics Letters* 2016; 108(17): 171905. doi: 10.1063/1.4947577
64. Zhong C, Li J, Lin H. Graphene-based all-optical modulators. *Frontiers of Optoelectronics* 2020; 13(2): 114–128. doi: 10.1007/s12200-020-1020-4
65. Zhang X, Zhang B, Sun M, et al. Preparation and thermal conductivity properties of high-temperature resistance polyimide composite films based on silver nanowires-decorated multi-walled carbon nanotubes. *Journal of Materials Science: Materials in Electronics* 2022; 33: 1577–1588. doi: 10.1007/s10854-021-07680-x
66. Chan CH, Wu TY, Yen MH, et al. Low power consumption and high-contrast light scattering based on polymer-dispersed liquid crystals doped with silver-coated polystyrene microspheres. *Optics Express* 2016; 24(26): 29963–29971. doi: 10.1364/OE.24.029963
67. Kim H, Inoue Y, Kobashi J, et al. Deformation-free switching of polymer-stabilized cholesteric liquid crystals by low temperature polymerization. *Optical Materials Express* 2016; 6(3): 705–710. doi: 10.1364/OME.6.000705